

# Road Surface Condition Identification with Deep Neural Networks and SVM Classifier

**R. Ramya Krishna**

Department of EECE, GITAM (Deemed to be University), Visakhapatnam, India  
ramyakrishnarajavolu9@gmail.com (corresponding author)

**N. Jyothi**

Department of EECE, GITAM (Deemed to be University), Visakhapatnam, India  
jnutakki@gitam.edu

Received: 9 January 2025 | Revised: 29 January 2025 and 25 February 2025 | Accepted: 27 February 2025

Licensed under a CC-BY 4.0 license | Copyright (c) by the authors | DOI: <https://doi.org/10.48084/etasr.10166>

## ABSTRACT

Roads are people's main transportation mode, deeming them an important aspect of worldwide everyday life. However, weather conditions increasingly impact road infrastructure, necessitating improved road safety measures. Identifying road types enhances traffic management and safety, particularly as roads often sustain damage during the rainy season and require restoration that takes time. In many countries, weather conditions also affect road usability. This study proposes a Deep Neural Network (DNN) for automatic road classification Road Surface Images (RSI). ResNet-50 is employed for feature extraction, while additional features, such as Gray-Level Co-Occurrence Matrix (GLCM), correlation factor, and Histogram of Oriented Gradients (HOG) are integrated to improve detection accuracy. These features collectively form the GHR50 model. Next, the collected features are classified using a Support Vector Machine (SVM) classifier and the parameters are evaluated. The proposed GHR50 model achieves 97.39% accuracy in detecting road types, such as dry mud, fresh snow, and water-asphalt smooth, representing a 0.95% improvement over conventional Convolutional Neural Networks (CNNs).

*Keywords-road surface images; deep neural network; histogram of oriented gradient; grey level co-occurrence matrix; residual network; support vector machine*

## I. INTRODUCTION

Research on autonomous vehicles has significantly increased in recent years. These technologies could minimize traffic congestion, accidents, energy consumption, and environmental impact. A critical aspect of autonomous driving is image classification, which enhances road condition detection and improves safety. Road surfaces can vary widely, including muddy, slippery, snowy, dry, or wet conditions. However, factors, such as adverse weather, variable lighting, and motion blur, can reduce the clarity of RSI, negatively impacting traditional classification methods and leading to inconsistent accuracy and limited adaptability. Therefore, more robust and reliable classification techniques are needed for road surface condition assessment.

The foundation of modern image classification lies in neural network research. Authors in [1], who studied cat cerebral cortex neurons, important for local sensitivity and direction selection, postulated CNN in the 1960s. Authors in [2] used CNNs in character recognition in the 1990s to reduce feature extraction effort. Later, authors in [3] offered a classical CNN model for image recognition to help solve the tasks. The CNN strong performance lies in picture target recognition and classification [4]. However, improving classification accuracy

remains a key challenge. Researchers have explored alternative approaches, including color space features for image identification [5], and have modified SVMs for classification [6]. A system integrating these techniques achieved 85% accuracy in mixed road condition identification, though its effectiveness was limited by a small sample size. Deep Learning (DL) models, particularly CNNs, have greatly enhanced image classification performance. As DL methods continue to evolve, novel activation functions for DNNs are being explored [7]. Non-linear data processing remains challenging, as conventional models rely on linear convolution and fully connected layers. To address this, non-linear activation functions have been incorporated into network structures, enabling more complex feature mappings [8]. The Rectified Linear Unit (ReLU) function, proposed in [9], accelerates DNN training.

This study integrates DL and SVM for road surface classification, focusing on the impact of layer selection and activation functions on classification accuracy. The proposed approach is evaluated using publicly available road surface datasets, including a dataset from [10], containing 370,151 road RSI from China under various weather and road conditions. Figure 1 portrays RSI samples.

This paper makes two primary contributions:

- **Feature Extraction:** An enhanced ResNet-50 model is employed, along with HOG, GLCM, and correlation-based features.
- **Feature Classification:** An optimized SVM classifier is utilized to improve road surface condition recognition.

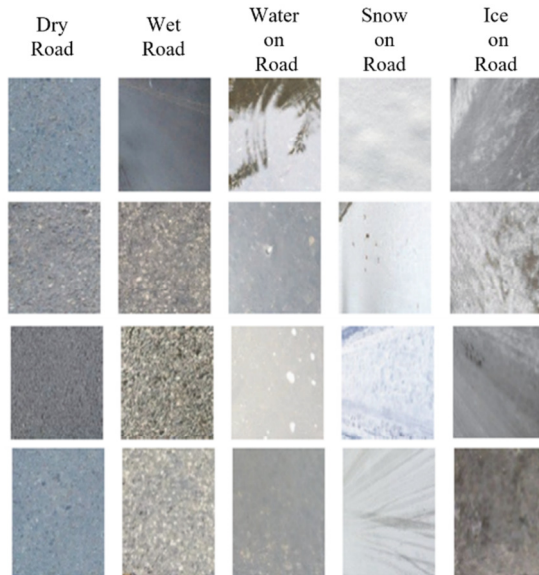


Fig. 1. RSI image samples.

## II. RELATED WORK

Traffic meteorology classifies roads as dry, wet, water, snow, or ice based on the liquid on their surfaces. Road surface-detecting sensors are now the main source of slippery road surface data. RSI are captured by sensors and analyzed to determine the road type. Various algorithms have been proposed for road surface recognition, initially relying on integrated tools [11] before transitioning to image-based processing techniques. Authors in [12] retrieved road image features and revealed road surface condition. A tire-road variability-based real-time acoustics road surface state identification system was proposed in [13]. Using a signal processing technique and a noise measuring device, dry and wet road statuses were accurately classified. Feature extraction was not performed, lowering accuracy. Authors in [14] proposed a technique using gray scale RSI characteristics and a neural network for road surface detection, demonstrating improved recognition. Authors in [15] investigated a large collection of road surface reflection images to monitor and identify the reflection image of a specific site. They also explained the relationship between the friction coefficient and surface roughness. A model using statistical features, GLCM, and linear discriminant analysis was presented in [16] for Road Surface Classification (RSC), emphasizing feature extraction as a critical step. Human-computer interaction techniques were employed in [17] to extract temperature and grayscale features for road surface prediction, achieving over 80% accuracy. Focusing on hazardous road conditions, authors in [18]

leveraged road brightness and RSI spatial spectrum data for classification. In [19], a Backpropagation (BP) neural network model was developed, incorporating RGB, HSI, and YUV color spaces to improve recognition accuracy above 85%. However, the model's effectiveness was limited by a small training dataset.

An SVM classifier was utilized in [20] to detect slippery roads using wet road images, showing slightly higher accuracy for snow than for dry conditions. Further research is needed to improve the classification of hybrid road surface states. A Recurrent Neural Network (RNN)-based approach was introduced in [21] to enhance wet/dry road classification using tire noise data, achieving 93% accuracy despite challenges caused from vehicle speed, environmental noise, and tire friction. In [22], a Deep Convolutional Neural Network (DCNN) model was developed to classify asphalt, cement, and blacktop surfaces under wet and dry conditions, reaching 92% accuracy. Further research is needed to enhance road surface data collection using mobile devices. A DCNN-based approach leveraging cellphone images was introduced in [23], demonstrating effective feature extraction using two fully connected layers. DL has been shown to improve road surface recognition for traffic flow. DenseNet and NASNet architectures were proposed in [24] to monitor winter road conditions, incorporating temperature, wind speed, humidity, pressure, and dew point data. Additionally, a LiDAR-based spatiotemporal framework was introduced in [25] to classify road surface materials (asphalt, cement, gravel, tarmac) and conditions (dry, wet, snowy) with approximately 97% accuracy. While most studies focus on isolated feature extraction techniques, this work integrates multiple feature extraction methods. By leveraging public datasets, it minimizes environmental noise while maintaining high image quality.

## III. METHODOLOGY

Four main steps are followed to determine road surface from photos, data acquisition, pre-processing, feature extraction, and classification. Figure 2 illustrates the utilized method.

### A. Input Dataset

Most publicly available datasets are photographs taken in constrained conditions, reducing algorithms' real-world robustness. A large dataset of RSI was labeled based on friction, substance, and unevenness attributes. The friction level categories—dry, wet, water, fresh snow, melting snow, and ice—correlate with various weather conditions. Road surfaces include gravel, mud, asphalt, and concrete, while road unevenness is classified as smooth, mild, or severe, depending on the environmental conditions. The dataset follows a structured classification, incorporating these three primary attributes along with their respective subcategories. However, when friction is classified as ice, melting snow, or fresh snow, the road substance and unevenness attributes are not emphasized. Authors in [10] divided the dataset's image categories into 27 subcategories, and similar subcategories were used in this work. The employed dataset, was obtained from [26] and was used for the evaluation of the proposed model.

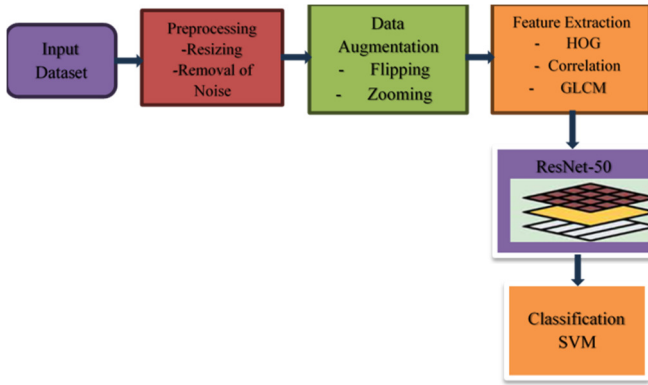


Fig. 2. Process flow of the proposed work.

### B. Pre-processing of Data

Before feeding images into a pre-trained model, they must undergo pre-processing. This stage includes downsizing, noise removal, data augmentation, and color conversion to greyscale. Additionally, all data must be uniformly scaled before testing. The images are resized from  $240 \times 360$  pixels (96 DPI) to  $224 \times 224 \times 3$  pixels. Noise is removed using a median filter, and data augmentation is applied to prevent class imbalance, ensuring seamless training for Machine Learning (ML) and DL models. The augmentation techniques include rotation, scaling, and translation. After augmentation, color images are converted to greyscale for better feature extraction. Finally, all images are normalized using pre-trained model norms.

### C. Feature Extraction

Feature extraction is a crucial step in image processing applications. The primary feature extraction techniques deployed are GLCM, HOG, and DCNN.

#### 1) Gray-Level Co-Occurrence Matrix Features

GLCM is a widely used method for analyzing image textures by examining pixel relationships. The extracted GLCM features include:

- Contrast: Measures variations in pixel intensity. High contrast indicates significant differences between neighboring pixels:

$$\text{Contrast} = \sum_{i,j} (i - j)^2 \cdot P(i, j) \quad (1)$$

where the  $P(i, j)$  is the value in GLCM for  $i$  and  $j$  pixels.

- Energy: The GLCM uniformity is measured using the energy factor. Higher energy values indicate more repetitive and structured textures:

$$E = \sum_{i,j} P(i, j)^2 \quad (2)$$

- Homogeneity: Measures how close the elements in the GLCM are to the diagonal. Higher values indicate a more uniform distribution:

$$H = \sum_{i,j} \frac{P(i, j)}{1 + |i - j|} \quad (3)$$

- Entropy: Evaluates the randomness of grey level distributions. Higher entropy implies more complex textures:

$$E_n = -\sum_{i,j} P(i, j) \log P(i, j) \quad (4)$$

- Dissimilarity: This feature varies and increases linearly depending on the grey levels in the image:

$$D_s = \sum_{i,j} |i - j| \cdot P(i, j) \quad (5)$$

- Cluster shade: Measures the asymmetry in the texture of the image. The matrix skewness is measured using the cluster shade:

$$CS = \sum_{i,j} (i + j - \mu_x - \mu_y)^3 \cdot P(i, j) \quad (6)$$

- Cluster prominence: Measures the peak distribution function of the image. The matrix kurtosis is evaluated:

$$CP = \sum_{i,j} (i + j - \mu_x - \mu_y)^4 \cdot P(i, j) \quad (7)$$

- Maximum probability: Every image has a pair of pixels which are relevant. This parameter is used to evaluate the most common suitable pair of pixels:

$$MP = \max(P(i, j)) \quad (8)$$

- Sum of squares: The variance around the GLCM factor is evaluated. This involves the mean function:

$$SOS = \sum_{i,j} (i - \mu)^2 \cdot P(i, j) \quad (9)$$

#### 2) Correlation

Apart from all the GLCM features extracted, correlation is one of the most important factors. The pixels available in the image are correlated with the neighbor image pixels and with entire dataset images. The values of correlation range from -1 to 1. If the value is 1, the pixels are highly correlated, whereas if it is -1, the pixels are uncorrelated. If the value ranges from 0.4 to 0.8 then the pixels are said to be positively correlated. The evolution of correlation is given by:

$$\text{Corr} = \sum_{i,j} \frac{i \cdot j \cdot P(i, j) - \mu_x \mu_y}{\sigma_x \sigma_y} \quad (10)$$

where  $\mu_x$ ,  $\mu_y$  represent the mean and  $\sigma_x$ ,  $\sigma_y$  the standard deviation of the marginal distributions of  $P(i, j)$ .

#### 3) Histogram of Gradient Features

HOG is used to extract the edge and shape features of road surfaces. The process includes:

- Dividing the image into small cells and computing gradient directions for each.
- Grouping pixels into angular bins based on gradient direction.
- Weighting pixels and assigning them to respective angular bins.
- Combining adjacent cells into blocks for normalization.
- Constructing the HOG descriptor from the block histograms.

Using (11)-(12), 2D gradient is determined for every pixel  $(X_i, Y_j)$  in the given input image. Equation (13) is utilized to find gradient magnitude and (14) to determine the gradient angle:

$$GRX = Imp(X_i + 1, Y_j) - Img(X_i - 1, Y_j) \quad (11)$$

$$GRY = Imp(X_i, Y_j + 1) - Img(X_i, Y_j - 1) \quad (12)$$

$$GR(X, Y) = \sqrt{GRx^2 + GRy^2} \quad (13)$$

$$\tan(\varphi(X, Y)) = \frac{GRx}{GRy} \quad (14)$$

#### 4) Deep Convolutional Neural Network Features

Feature extraction is further enhanced using a DCNN, specifically the ResNet-50.

CNNs work exceptionally in object recognition, image classification, and road surface analysis. They consist of three primary layers:

- Convolutional Layer: Extracts feature maps from the input image.
- Pooling Layer: Reduces dimensionality, retaining only strong features.
- Fully Connected (FC) Layer: Uses extracted features for final classification.

The CNN model for the specified task is shown in Figure 3. One significant distinction between the ResNet-50 architecture and other designs is the usage of a three-layer stack. After extracting all the image features, the latter are fed to the SVM classifier and surface identification proceeds.

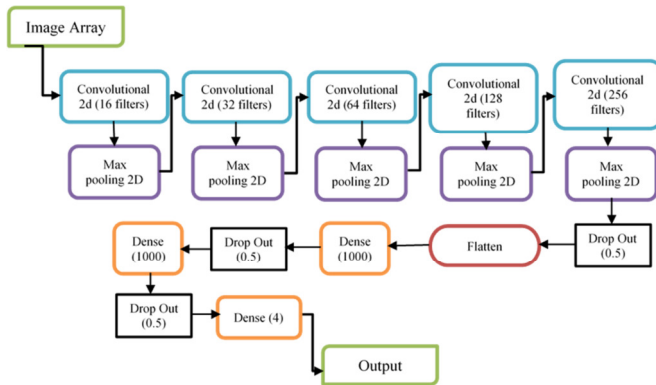


Fig. 3. Proposed CNN model.

#### D. Support Vector Machine

The goal of SVM is to locate the best hyperplane that maximizes the distance on both sides of the hyperplane. SVM also guarantees the correctness of the hyperplane categorization. The identification of hybrid road surface conditions is accomplished using a nonlinear multiclass SVM classifier.

The nonlinear transformation from the kernel functionality to input space determines the nonlinear-to-linear

transformation. The hyperplane fulfills the following requirement and divides the data into two groups:

$$WX + b = 0 \quad (15)$$

where  $X$  is the hyperplane's support vector, or the data from each group that are closest to the hyperplane, and  $W$  is the hyperplane's normal vector.

The dataset consists of 370,151 samples, with 70% being allocated for training and 30% for testing.

#### IV. RESULTS AND DISCUSSION

The proposed device uses 64bit-OS, 16gb RAM, Intel i7 processor, and NVIDIA graphic card. The designed network is trained and evaluated employing DNN toolbox. The step-by-step technique outcomes are displayed in Figure 4. The last three layers of ResNet-50 are replaced by fully linked, softmax, and classification layers. The SVM classifier showed promising road surface identification results. The training and testing of the model facilitated the identification of the desired outcomes. Most road surface detection techniques use the DCNN model. The test results demonstrate that the input image type greatly affects learning accuracy.

The metrics evaluated are sensitivity, specificity, precision, and accuracy. These metrics are calculated using four notations: True Positives ( $TP$ ), representing correctly predicted instances, False Positives ( $FP$ ) representing misclassified instances, True Negatives ( $TN$ ) representing correctly identified general images, and False Negatives ( $FN$ ) representing instances misclassified as normal. The model is designed to use ground truth images for comparison with the given input test image to evaluate the metrics.

- Sensitivity: The proportion of  $TP$  correctly identified for a given input, also known as recall or the  $TP$  rate. It is calculated as:

$$Se = \frac{TP}{TP + FN} \quad (16)$$

- Specificity: The proportion of  $TN$  correctly identified, also known as the  $TN$  rate. It is calculated as:

$$Sp = \frac{TN}{TN + FP} \quad (17)$$

- Precision: The proportion of correctly predicted positive instances out of all predicted positives. It is calculated as:

$$Precision = \frac{TP}{TP + FP} \quad (18)$$

- Accuracy: A measure combining both systematic and random errors, requiring both trueness and precision. It is calculated as:

$$Ac = \frac{TP + TN}{TP + TN + FP + FN} \quad (19)$$

Table I presents the evaluated parameters for the CNN model against those of the proposed DL model. The results indicate that the proposed model displays an improvement of 1% across these metrics.

TABLE I. PARAMETRIC EVALUATION

Parameter/Model	CNN	GHR50-SVM
Accuracy (%)	96.44	97.39
Sensitivity (%)	96.43	97.40
Specificity (%)	96.21	97.18
Precision (%)	96.32	97.28

Figures 5 and 6 illustrate the confusion matrix, which provides a visual interpretation of the model's classification performance. The confusion matrix compares the predicted values with the actual values, calculating the percentage of misclassified predictions. This approach is deployed to assess the classification accuracy of each multi-class classifier on both training and test data.

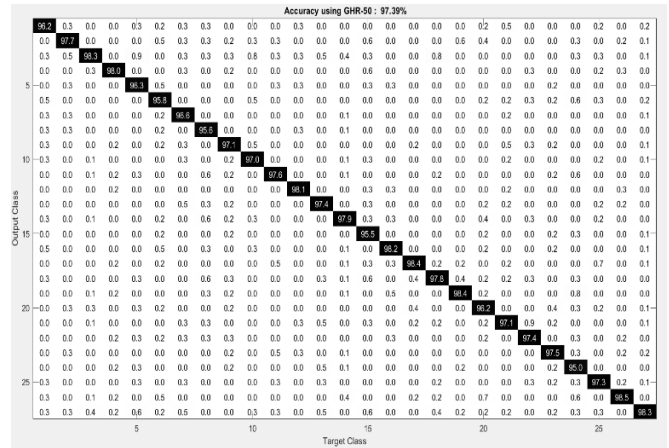


Fig. 6. Confusion matrix using GHR50-SVM.

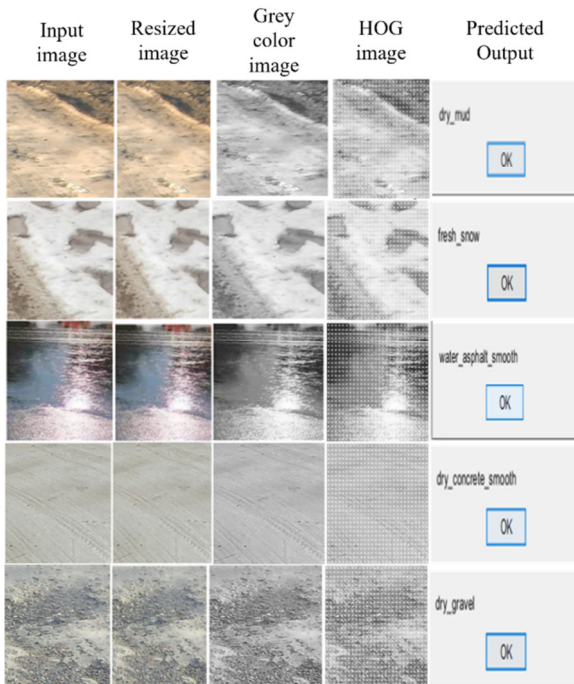


Fig. 4. The step-by-step technique outcomes of the proposed model.

TABLE II. COMPARISON WITH EXISTING TECHNIQUES

Author & Year	Technique	Accuracy (%)
[27] (2012)	Canny Edge + Hough Transform	90.0
[28] (2013)	SVM	88.0
[29] (2017)	PSO + SVM	90.0
[30] (2019)	New ReLU DL approach	94.98
[23] (2020)	VGG + SVM	91.80
[31] (2023)	R101-FPN Model	92.5
[32] (2024)	MLP DL approach + MM Transform	95.6
Proposed	GHR50-SVM	97.39

The proposed model outperformed existing techniques in terms of accuracy, as detailed in Table II. Table II provides the ratio of the correctly predicted road surface conditions to the total number of predictions, indicating the accuracy of each classification. The rightmost section of Table II displays the proportion of the correctly identified road surface conditions relative to those that were misclassified, representing the accuracy of each true class.

V. CONCLUSION

Deep Convolutional Neural Networks (DCNN) possess strong recognition and learning capabilities. Their application in real-time Road Surface Classification (RSC) provides valuable information for maintenance teams, enabling rapid and effective responses to hazardous conditions. DCNN and Machine Learning (ML) models are highly effective in image recognition and classification tasks.

In this study, feature extraction techniques, such as the Gray-Level Co-Occurrence Matrix (GLCM), correlation factors, and the Histogram of Oriented Gradients (HOG) were utilized to identify different road surface conditions. Additionally, ResNet-50 was employed for feature extraction. Finally, a Support Vector Machine (SVM) classifier was used for road surface classification. The evaluation results indicate that the proposed GHR50-SVM methodology achieved a superior accuracy rate compared to standard Convolutional Neural Networks (CNN), attaining an accuracy of 97.39%. The findings suggest that a data-driven learning model capable of predicting road conditions with accuracy comparable to cost-

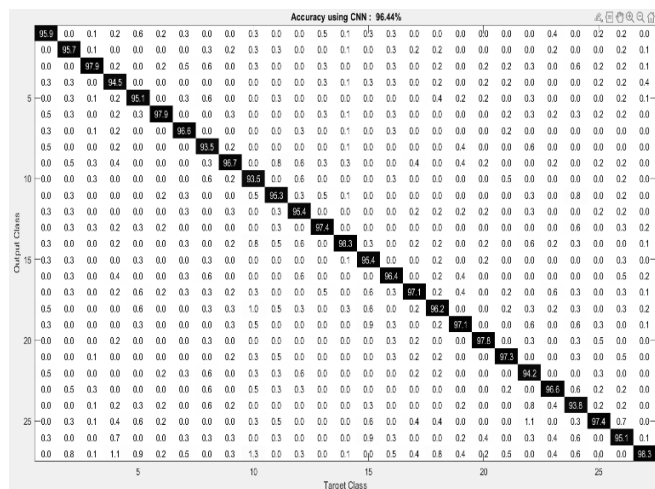


Fig. 5. Confusion matrix using CNN.

intensive detectors can be developed, provided that relevant weather and road surface data are available. This study focused exclusively on Deep Learning (DL) and SVM classifiers to demonstrate the feasibility of using data-driven models for the road surface condition prediction under adverse weather conditions. Future research should explore additional DL models and ensemble ML techniques to further enhance predictive performance. Furthermore, as road surface characteristics are highly influenced by weather conditions, additional factors related to pavement properties should be incorporated into future models.

## REFERENCES

- [1] T. N. Wiesel and D. H. Hubel, "Effects of Visual Deprivation on Morphology and Physiology of Cells in the Cat's Lateral Geniculate Body," *Journal of Neurophysiology*, vol. 26, no. 6, pp. 978–993, Nov. 1963, <https://doi.org/10.1152/jn.1963.26.6.978>.
- [2] Y. Lecun, L. Bottou, Y. Bengio, and P. Haffner, "Gradient-based learning applied to document recognition," *Proceedings of the IEEE*, vol. 86, no. 11, pp. 2278–2324, Nov. 1998, <https://doi.org/10.1109/5.726791>.
- [3] A. Krizhevsky, I. Sutskever, and G. E. Hinton, "ImageNet classification with deep convolutional neural networks," *Communications of the ACM*, vol. 60, no. 6, pp. 84–90, May 2017, <https://doi.org/10.1145/3065386>.
- [4] D. Doan Van, "Application of Advanced Deep Convolutional Neural Networks for the Recognition of Road Surface Anomalies," *Engineering, Technology & Applied Science Research*, vol. 13, no. 3, pp. 10765–10768, Jun. 2023, <https://doi.org/10.48084/etasr.5890>.
- [5] Z. Liu, J. Yang, and C. Liu, "Extracting Multiple Features in the CID Color Space for Face Recognition," *IEEE Transactions on Image Processing*, vol. 19, no. 9, pp. 2502–2509, Sep. 2010, <https://doi.org/10.1109/TIP.2010.2048963>.
- [6] S. Zhang, S. Zhao, Y. Sui, and L. Zhang, "Single Object Tracking With Fuzzy Least Squares Support Vector Machine," *IEEE Transactions on Image Processing*, vol. 24, no. 12, pp. 5723–5738, Dec. 2015, <https://doi.org/10.1109/TIP.2015.2484068>.
- [7] Y. Liu, Y. Cheng, and W. Wang, "A survey of the application of deep learning in computer vision," in *Global Intelligence Industry Conference (GIIC 2018)*, Beijing, China, Aug. 2018, p. 68, <https://doi.org/10.1117/12.2505431>.
- [8] D. Erhan, Y. Bengio, A. Courville, P.-A. Manzagol, P. Vincent, and S. Bengio, "Why Does Unsupervised Pre-training Help Deep Learning?," *J. Mach. Learn. Res.*, vol. 11, pp. 625–660, Mar. 2010.
- [9] P. Petersen and F. Voigtlaender, "Optimal approximation of piecewise smooth functions using deep ReLU neural networks," *Neural Networks*, vol. 108, pp. 296–330, Dec. 2018, <https://doi.org/10.1016/j.neunet.2018.08.019>.
- [10] T. Zhao and Y. Wei, "A road surface image dataset with detailed annotations for driving assistance applications," *Data in Brief*, vol. 43, Aug. 2022, Art. no. 108483, <https://doi.org/10.1016/j.dib.2022.108483>.
- [11] L. Cai, D. C. Zhang, B. Li, L. D. Gao, and L. Wang, "Traffic meteorological embedded road conditions detector test method research," *Road Traffic and Safety*, vol. 14, no. 6, pp. 55–59, 2014.
- [12] Z. Qi, B. Wang, X. Pei, and G. Ma, "A method of road surface identification based on road characteristics and the features of antilock braking adjustment," *Qiche Gongcheng/Automotive Engineering*, vol. 36, pp. 310–315, Mar. 2014.
- [13] W. Chinkhuntha, A. Owayo, and N. Ambassah, "Performance Evaluation of Red Clay Soils stabilized with Bluegum Sawdust Ash and Sisal Fiber as Low-Volume Road Sub-base Materials," *Engineering, Technology & Applied Science Research*, vol. 14, no. 6, pp. 18105–18113, Dec. 2024, <https://doi.org/10.48084/etasr.8772>.
- [14] A. Kuehnle and W. Burghout, "Winter Road Condition Recognition Using Video Image Classification," *Transportation Research Record: Journal of the Transportation Research Board*, vol. 1627, no. 1, pp. 29–33, Jan. 1998, <https://doi.org/10.3141/1627-05>.
- [15] A. B. Slimane, M. Khoudeir, J. Brochard, and M.-T. Do, "Characterization of road microtexture by means of image analysis," *Wear*, vol. 264, no. 5–6, pp. 464–468, Mar. 2008, <https://doi.org/10.1016/j.wear.2006.08.045>.
- [16] Y. Chen, "Image analysis applied to black ice detection," presented at the Orlando '91, Orlando, FL, Orlando, FL, Mar. 1991, pp. 551–562, <https://doi.org/10.1117/12.45497>.
- [17] I. Yamamoto, M. Kawana, I. Yamazaki, H. Tamura, and Y. Ookubo, "The Application of Visible Image Road Surface Sensors to Winter Road Management," in *Proceedings of the 12th World Congress on Intelligent Transport Systems*, San Francisco California, United States, Nov. 2005.
- [18] D. Patil and S. Jadhav, "Road Segmentation in High-Resolution Images Using Deep Residual Networks," *Engineering, Technology & Applied Science Research*, vol. 12, no. 6, pp. 9654–9660, Dec. 2022, <https://doi.org/10.48084/etasr.5247>.
- [19] H. Li, Y. H. Feng, and J. Lin, "Study on road surface condition identification based on BP network improved," *Microcomputer Information*, vol. 26, no. 2, pp. 3–4, 2010.
- [20] X. Y. Liu and Q. D. Huang, "Study on classifier of wet road images based on SVM," *Journal of Wuhan University of Technology (Transportation Science and Engineering)*, vol. 35, no. 4, pp. 784–787, 2011.
- [21] I. Abdic *et al.*, "Detecting road surface wetness from audio: A deep learning approach," in *2016 23rd International Conference on Pattern Recognition (ICPR)*, Cancun, Dec. 2016, pp. 3458–3463, <https://doi.org/10.1109/ICPR.2016.7900169>.
- [22] M. Nolte, N. Kister, and M. Maurer, "Assessment of Deep Convolutional Neural Networks for Road Surface Classification," 2018, <https://doi.org/10.48550/ARXIV.1804.08872>.
- [23] J. Carrillo, M. Crowley, G. Pan, and L. Fu, "Design of Efficient Deep Learning models for Determining Road Surface Condition from Roadside Camera Images and Weather Data," 2020, <https://doi.org/10.48550/ARXIV.2009.10282>.
- [24] J. Carrillo and M. Crowley, "Integration of Roadside Camera Images and Weather Data for Monitoring Winter Road Surface Conditions," 2020, <https://doi.org/10.48550/ARXIV.2009.12165>.
- [25] J. W. Seo, J. S. Kim, and C. C. Chung, "Classification Method of Road Surface Condition and Type with LiDAR Using Spatiotemporal Information," *arXiv*, Aug. 11, 2023, <https://doi.org/10.48550/arXiv.2308.05965>.
- [26] Tong Zhao, "Road Surface Image Dataset with Detailed Annotations," *Mendeley*, Jul. 11, 2022, <https://doi.org/10.17632/W86HVKRZC5.2>.
- [27] A. Raj, D. Krishna, R. Hari Priya, K. Shantanu, and S. Niranjani Devi, "Vision based road surface detection for automotive systems," in *2012 International Conference on Applied Electronics*, 2012, pp. 223–228.
- [28] K. J. Hoon, and W. J. Moo, "A Development of The Road Surface Decision Algorithm Using SVM (Support Vector Machine) Clustering Methods," *The Journal of The Korea Institute of Intelligent Transport Systems*, vol. 12, no. 5, pp. 1–12, Oct. 2013, <https://doi.org/10.12815/kits.2013.12.5.001>.
- [29] J. Zhao, H. Wu, and L. Chen, "Road Surface State Recognition Based on SVM Optimization and Image Segmentation Processing," *Journal of Advanced Transportation*, vol. 2017, pp. 1–21, 2017, <https://doi.org/10.1155/2017/6458495>.
- [30] L. Cheng, X. Zhang, and J. Shen, "Road surface condition classification using deep learning," *Journal of Visual Communication and Image Representation*, vol. 64, Oct. 2019, Art. no. 102638, <https://doi.org/10.1016/j.jvcir.2019.102638>.
- [31] S. Lee, J. Jeon, and T. H. M. Le, "Feasibility of Automated Black Ice Segmentation in Various Climate Conditions Using Deep Learning," *Buildings*, vol. 13, no. 3, Mar. 2023, Art. no. 767, <https://doi.org/10.3390/buildings13030767>.
- [32] Y. Moroto, K. Maeda, R. Togo, T. Ogawa, and M. Haseyama, "Multimodal Transformer Model Using Time-Series Data to Classify Winter Road Surface Conditions," *Sensors*, vol. 24, no. 11, May 2024, Art. no. 3440, <https://doi.org/10.3390/s24113440>.